JOURNAL OF APPLIED ELECTROCHEMISTRY 22 (1992) 82–86

X-ray diffraction study of anisotropy by the formation and decomposition of nickel hydride
Part II: Decomposition kinetics

I. TOMOV, M. MONEV, M. MIKHAILOV, S. RASHKOV

Institute of Physical Chemistry, Bulgarian Academy of Sciences, 1040 Sofia, Bulgaria

Received 16 October 1990; revised 14 April 1991

The role of the microstructure on the decomposition of β-NiH formed as a result of the H cathodic charging of nickel was studied with the help of X-ray diffraction methods. This decomposition follows Kolmogorov-Avrami-Johnson-Mehl kinetics. The microstructural anisotropy induces anisotropy in the rate of phase transformation which is governed by the chemical reaction β-NiH $\rightarrow$ Ni + H, i.e. it proceeds without diffusion limitations.

1. Introduction

The chemical decomposition of β-NiH is a typical example of a topochemical or solid-state reaction. The kinetic analysis of the decomposition of β-NiH, obtained as a result of cathodically charging Ni with H, was carried out using volumetric [1] and X-ray diffraction (XRD) [2–6] methods. Most of these indicated that β-NiH decomposition is, as a rule, a first-order reaction [1–5], but there is also a case presented [6] in which the β-NiH decomposition is described by a different distribution function. These results [1–5] are irreconcilable with the regularities in the kinetics which have been observed in the formation and decomposition of metal hydrides [7, 8].

On the grounds that the time of decomposition of NiH, formed in polycrystalline specimens, is considerably less than in single crystals, it is assumed in [9] that the NiH life-time is dependent on the crystal size. The role of the dislocations in β-NiH formation and decomposition has been discussed in [3]. Our previous study [10] shows that the extent of phase transformation of Ni into β-NiH is a function of many parameters, which are dependent on the crystal direction and microstructure of nickel. In principle, the real structure determines the solid-state transformation rate by its influence both on the chemical decomposition rate (by means of the various defects in the crystal lattice), and on the rate with which the gaseous product leaves the reaction zone, i.e. the diffusion rate [11].

There have been no studies as yet on the effect of the microstructure (crystal size and microdeformations) on β-NiH decomposition. But the microstructure is an anisotropic property of materials [12]. The purpose of the present study was to acquire information on the influence of microstructure anisotropy on the β-NiH decomposition rate in the various crystal directions. For such intentions XRD is a suitable tool for the selective investigation of the transformations in the two-phase system of α-NiH and β-NiH.

2. Experimental details

The models for the present study were the same as those employed in [10], where the conditions for their preparation and hydrogen charging are fully described.

The changes in the β-NiH volume fractions (which are a measure of the extent of phase transformation) with time were followed with the use of Cu_α-radiation. The time for measuring the integrated intensity (area) of each diffraction line was 100 s, i.e. it is negligible compared to the experimentally established time of full decomposition of the β-NiH phase. Thus the NiH volume fractions were not noticeably influenced by any effects which might arise from the measuring equipment. XRD offered a possibility for the direct investigation for the rate of phase transformation, occurring in the surface layer with a thickness equal to the effective depth of X-ray penetration [13, 14].

3. Results and discussion

3.1. *Decomposition kinetics of β-NiH at room temperature*

To assess the influence of the microstructure anisotropy on β-NiH decomposition, models were employed with considerably differing microstructures which have arisen either after electrodeposition, or were a result of recrystallization after annealing processes. Data on the microstructure of unannealed specimens is presented in our previous paper (Table 2 in [10] in which the numbering of the specimens is identical with the present paper).

It is well known that the kinetic behaviour exhibited by hydriding and dehydriding processes [7, 8, 15] is similar to that of many phase transformations of the

0021-891X/92 $03.00 + .12

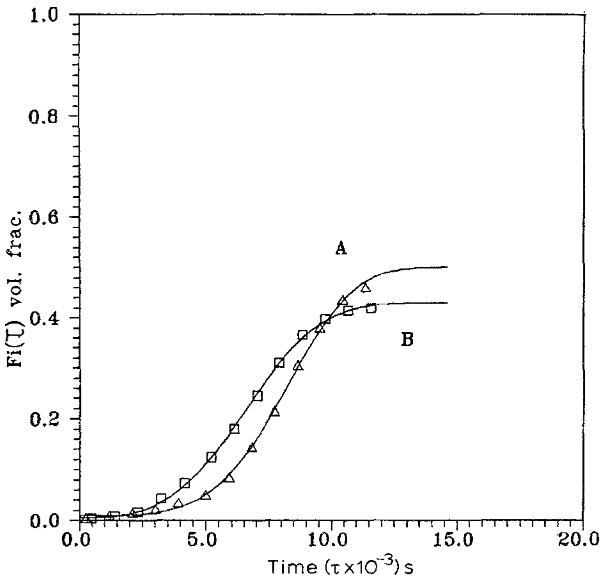

Fig. 1. Anisotropy in the kinetics of decomposition of β-NiH, formed in electrodeposited matt nickel (specimen No. 1). $F_i(\tau)$: volume fraction of the nickel hydride which has decomposed in the ⟨1 1 1⟩ (A) and ⟨1 0 0⟩ (B) directions.

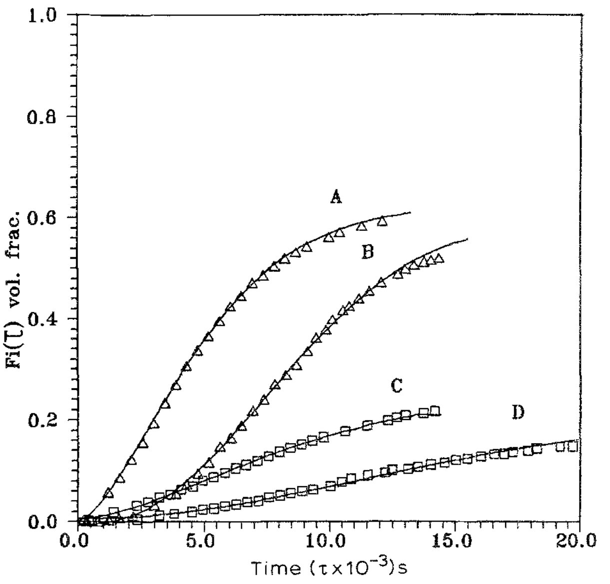

Fig. 2. Anisotropy in the kinetics of decomposition of β-NiH, recrystallized after thermally treating Ni (specimen No. 3′). $F_i(\tau)$: volume fraction of the hydride which has decomposed in the ⟨1 1 1⟩ and ⟨1 0 0⟩ directions and formed as a result of cathodic charging with H both in the absence (curves A and C, respectively) and presence of Cu^{2+} (curves B and D, respectively).

nucleation and growth type, i.e. the summary transformation process is described by the equation of Kolmogorov [16], Avrami [17], Johnson and Mehl [18]

$$F_i(\tau) = f_i\left\{1 - \exp\left[-\left(\frac{\tau}{\tau_i}\right)^k\right]\right\} \qquad (1)$$

where $F_i(\tau)$ is the β-NiH volume fraction corresponding to the i-direction, decomposed to time τ, i.e.

$$F_i(\tau) = f_i - f_i(\tau) \qquad (2)$$

f_i is the β-NiH fraction at $\tau = 0$ (i.e. the fraction which has formed up to the cessation of cathodic charging with H), $f_i(\tau)$ is the fraction present at the time τ, recorded after discontinuing the H charging, k is a number, the value of which is dependent on the geometry linked with the rate-controlling process, τ_i is the reaction rate time constant. The last term has a clear physical sense – this is the time $\tau = \tau_i$, for which the decomposed volume fraction $F_i(\tau)$ is related to the original fraction f_i by a constant factor

$$F_i(\tau_i) = \frac{e-1}{e}f_i = 0.6322\,f_i, \qquad (3)$$

which follows from Equation 1. The $f_i(\tau)$ fractions were calculated with the help of Equation 1 of [10]. The values of the parameters f_i, τ_i, and k were determined by computer fitting of the $F_i(\tau)$ relations (1) to the experimental data.

The values of exponent k are within the interval 1.5–4, the lower values pertaining to recrystallized large crystalline specimens and the greater values referring to unannealed fine crystalline specimens.

An illustration for the anisotropy of the decomposition kinetics in the ⟨1 1 1⟩ and ⟨1 0 0⟩ directions of an unannealed matt coating is given by Fig. 1. The differences in the induction periods and in the slopes of the self-accelerating parts of the two sigmoid curves are evident. An example for a decomposition in the same directions of NiH (curves A and C, respectively) formed in the recrystalized specimen No. 3′ (obtained after heat treatment of specimen No. 3) is presented in Fig. 2. The next two decomposition curves (C and D) in Fig. 2 were obtained after charging the same specimen with H in the presence of 10^{-7} M dm^{-3} Cu^{2+}. This experiment aimed to differentiate the influence of the various stages of β-NiH decomposition and the diffusion of H through α-Ni on the phase transformation.

The H diffusion occurs through the grain and twin boundaries, dislocations and non-defect parts of the crystalline lattice. It can be diminished to a certain extent by decorating the dislocations and grain and twin boundaries, which are paths for facilitated diffusion [19, 20]. This occurs during cathodic charging with H in the presence of small quantities of Cu^{2+} in the electrolyte [21], as a result of which copper is deposited preferentially on the emergency points of the dislocations and grain boundaries (i.e. active sites) on the surface. The comparison of the decomposition kinetics of the hydride, formed in the absence and presence of Cu^{2+} on one and the same specimen (i.e. under otherwise equal conditions – unchanged structure), is a proper approach for evaluating the role of the diffusion process for the rate of dehydriding. The similarity in the shape of the two pairs of curves (A, C) and (B, D) in Fig. 2 suggests that the change in the diffusion rate has no effect on the transformation mechanism. Therefore, the chemical reaction, not the diffusion, is the rate-limiting process. A confirmation of the conclusion that the phase transformation proceeds without any diffusion limitations follows from thermodynamic considerations: the activating energy of the β-NiH decomposition amounts to 61.5 kJ mol^{-1} [4], while that of diffusion is 39.7 kJ mol^{-1} [22], i.e. the latter is about 40% lower.

The integral kinetic curves for both crystal directions,

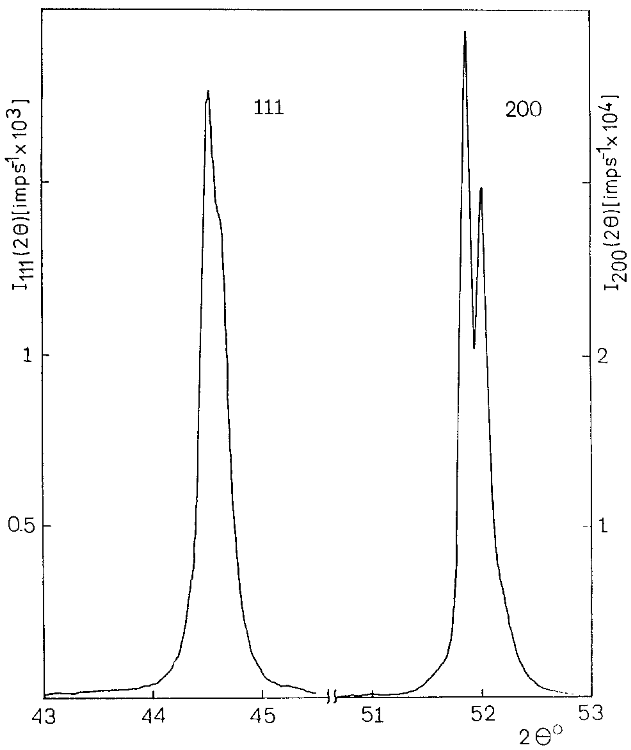

Fig. 3. Profile of the diffraction lines 111 and 200 of specimen No. 3′, after the decomposition of β-NiH.

shown in Fig. 2, differ considerably. The different forms of the A and C curves (as well as B and D) suggests that the topochemical reaction considerably differs in the ⟨1 1 1⟩ and ⟨1 0 0⟩ directions of specimen No. 3′. An explanation of this difference is offered by the analysis of Prodon for the influence of the ratio between surface and bulk localization of topochemical reactions on the form of the kinetic curve [23]. Topochemical reactions are, as a rule, localized on active sites on the surface and in the bulk of the crystal (spot bulk localization) [11, 23]. If the reaction occurs predominantly on the surface, the interface advance in the crystallite bulk results in a progressive decrease in the area of the reaction zone, leading to the absence of a self-acceleration part of the part of the respective kinetic curve. Where the surface and bulk localization are commensurate, the integral kinetic curve has a self-acceleration part. The spot bulk localization proceeds by the branching of the reaction and its selective permeation along dislocations in the crystal bulk [11]. Thus the ratio between the surface and bulk localization is determined by the ratio of the density and effectiveness of the active centres (micro- and macrodefects) on the surface and bulk of the crystallites. The above suggests that the kinetic curve shape is a consequence of the crystallite microstructure in the relevant crystal directions.

A qualitative assessment of the microstructure in the ⟨1 1 1⟩ and ⟨1 0 0⟩ directions of specimen No. 3′ can be made from the profile of the (1 1 1) and (2 0 0) diffraction lines, measured after the decomposition of β-NiH (Fig. 3). The doublet profile (with resolved components K_{α_1,α_2}) of the 200 line corresponds to large crystallites with a ⟨1 0 0⟩ orientation, in which the microdeformations are below the sensitivity of this measurement method, while there is no resolution of the α_1, α_2 doublet for the (1 1 1) line. The last is an indication for relatively higher microdeformations in crystallites with an ⟨1 1 1⟩ orientation. Pielaszek has also established that there are no isotropic deformations generated during the hydride formation-decomposition cycle (neither are there any deformations in the ⟨1 0 0⟩ direction [14]). Hence the shape observed of curve C (Fig. 2) with a just noticeable self-acceleration part, reflecting the predominance of the linear rate of interface advance over the bulk decomposition rate in the ⟨1 0 0⟩ direction. The relatively greater microdeformations due to defects in the interior of crystallites with ⟨1 1 1⟩ orientation, known to be generated during the charging with H [21], are a possible reason for the linear rate of interface advance and the bulk decomposition rate to be commensurate. This would explain the sigmoid shape of the A curve. In between these curves a whole spectrum of such curves can fit, the form of which can be explained analogously.

3.2. *Anisotropy of the β-NiH decomposition rate*

The β-NiH decomposition rate can be derived by differentiating Equation 1

$$\frac{\mathrm{d}F_i(\tau)}{\mathrm{d}\tau} = Q_i(\tau) = kf_i\left(\frac{1}{\tau_i}\right)^k \tau^{k-1} \exp\left[-\left(\frac{\tau}{\tau_i}\right)^k\right] \tag{4}$$

For the studied directions of all specimens this rate can be assessed by means of its value at the point of inflection ($Q_{\max}$). $Q_{\max}$ is the NiH volume fraction, which has undergone transformation per unit time, at the moment the maximum process rate is achieved. These values are presented in Table 1*. They are considerably higher for the large crystalline (matt and annealed) specimens, than for the fine crystalline (bright) specimens which have large microdeformations (see Table 3 in [10]). The diffeent $Q_{\max}$ in the various i-crystal directions for a given specimen are evidence that there is an anisotropy in the decomposition rate, which may depend on both crystal direction and Ni microstructure.

To evaluate the effect of microstructure alone on the dehydriding rate $Q_i(\tau)$, Fig. 4 compares kinetic data on the ⟨1 1 1⟩ crystal direction for specimens with considerably differing microstructures (Nos. 1, 5, 6 – see Table 3 in [10]). The differential kinetic curves $Q_i(\tau)$ were calculated according to Equation 4, in which the parameters f_i, τ_i and k were determined by fitting Equation 1 to the respective experimental data. Since the comparison was made for crystallographically equivalent directions, the difference observed between the curves is caused by the influence of the various microstructures on the phase transformation rate. The life-time of the hydride phase is greatest for specimen

---

* The $Q_{\max}$ values refer primarily for the ⟨1 1 1⟩ and ⟨1 0 0⟩ directions of the specimens. As a result of the presence of a texture as well as a low extent of phase transformation f_i in the ⟨1 1 0⟩ and ⟨3 1 1⟩ directions, no reliable results were obtained on the decomposition kinetics.

Table 1. Maximum decomposition rate $Q_{\max}$ (volume fraction per second) of β-NiH in the $\langle 1\,1\,1\rangle$, $\langle 1\,0\,0\rangle$ and $\langle 3\,1\,1\rangle$ directions of specimens with a $\langle \mu\,v\,w\rangle$ texture.

No.	$\langle \mu v w\rangle$	$Q_{\max} \times 10^5$ (vol. frac. $\times\ s^{-1}$)			Remark
		$\langle 111\rangle$	$\langle 100\rangle$	$\langle 311\rangle$	
1	100 + 221	8.9	7.2	–	matt unannealed
3	211 + 21	6.7	7.1	8.3	matt unannealed
3′	100 + 221	8.4	2.0	–	matt annealed
		5.7	1.1	–	Cu^{2+}
5	100 + 221	6.4	8.1	3.7	half-bright unannealed
6	111 + 100	3.6	3.2	2.8	bright unannealed
8′	100 + 111	5.4	3.9	2.1	metallurigical 99.7% purity annealed

No. 6, which has the highest microdeformations and the smallest crystallites (the largest area of grain boundaries). It is known that the defects and grain boundaries are sites which can act as H traps [24, 25]. On the basis of diffusion studies in [24], a list is given of the approximate values of the interaction energies between the trap and H atom for different trap types (point, line and planar trapping defects). The binding energy of trapping is lowest for point defects, and highest for dislocations, i.e. the last are the traps with the greatest depth. From such a point of view, the different differential curves in Fig. 4 can be explained by the varying density and efficiency of the traps. This effect reflects the expected microstructure influence (form and size of the crystallites and density of their defects) on the chemical reaction rate [11], which in fact, means on the hydride phase stability.

The intrinsic parameter for characterizing the NiH stability is the reaction time constant τ_i. This has been defined from the condition which follows from Equation 3. The τ_i values characterize the hydride stability at room temperature (Table 2). In the case of unannealed large crystalline specimens Nos. 1 and 3, the τ_i values are considerably lower than for fine crystalline coatings with large microdeformations, i.e. for the specimens Nos. 5 and 6. Hence it cannot be argued for a relationship between the NiH life-time and the crystallite size [9], without taking the microdeformations into account.

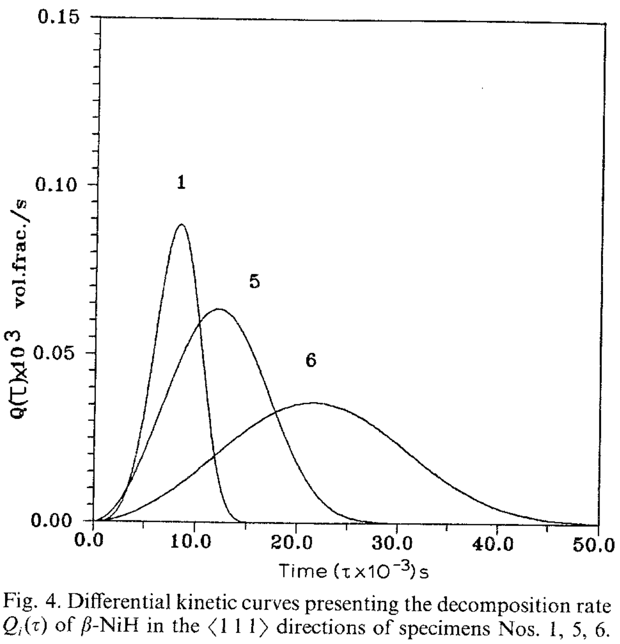

Fig. 4. Differential kinetic curves presenting the decomposition rate $Q_i(\tau)$ of β-NiH in the $\langle 1\,1\,1\rangle$ directions of specimens Nos. 1, 5, 6.

4. Conclusion

The kinetic analysis of β-NiH dehydriding indicates that the transformation rate is dependent on the structure of the medium where the chemical reaction proceeds. The experimental results can be treated from the standpoint that the chemical reaction is the rate-limiting stage in hydride decomposition. It has to be emphasized that the grain boundaries and dislocations may have a two-fold action on the phase transition: as shortened diffusion paths for the H transport, and a H traps [24, 25] by chemical reaction.

The conclusions may be drawn that the microstructure has a significant effect on the phase transition mechanism: for large crystal structures with a low defect density, the surface localization of the chemical reaction predominates; for fine crystal structures with a high defect density, the surface and spot bulk

Table 2. Reaction rate time constant τ_i in the $\langle 1\,1\,1\rangle$, $\langle 1\,0\,0\rangle$ and $\langle 3\,1\,1\rangle$ directions of specimens with different textures. D_k – current density at cathodic charging of nickel with hydrogen

No.	$D_k (A\ dm^{-2})$	$\tau_i (s)$		
		$\langle 111\rangle$	$\langle 100\rangle$	$\langle 311\rangle$
1	1	8860	7370	–
3	1	5990	5800	5160
3′	2	5545	9325	–
	1	9785	16420	–
5	1	13920	12870	14040
6	1	25015	24240	21440
8′	1.5	7325	5475	5925

localization are commensurate — the kinetic curves possess a significant self-acceleration part.

The discussed cases of β-NiH decomposition do not involve first order kinetics, as has been reported [1-5, 21].

Acknowledgements

The authors would like to thank Professor Dr Habil D. Kashchiev of the Institute of Physical Chemistry, Bulgarian Academy of Sciences, for his pertinent recommendations which helped the interpretation of the experimental results.

References

[1] B. Baranoswki, *Bull. Acad. Polon. Sci.* (*ser. sci. chim.*) **7** (1959) 891.

[2] A. Janko, *ibid.* **10** (1962) 617.

[3] J. Pielaszek, *ibid.* **20** (1972) 611.

[4] P. Ch. Borbe, F. Erdmann-Jesnitzer and W. Schoebel, *Z. Metallkunde* **71** (1980) 227.

[5] St. Rashkov, I. Tomov and A. Meltcheva, Nationalna Conferencia po Technologia na Galvanitchni Pokritia (proceedings), Sofia (1970), p. 25.

[6] St. Rashkov, M. Monev and I. Tomov, *Surf. Technology* **16** (1982) 203.

[7] J. W. Larsen and B. R. Livesay, *J. Less-Common Metals* **73** (1980) 79.

[8] I. G. Douglas and D. O. Northwood, *J. Mater. Sci.* **18** (1983) 321.

[9] A. Janko, *Bull. Acad. Polon. Sci.* (*ser. sci. chim*) **10** (1962) 613.

[10] I. Tomov and M. Monev, in preparation.

[11] B. Delmon, 'Introduction a la Cinetique Heterogene', (Russian transl.), Editions Technip., Paris (1969) pp. 379 and 413.

[12] H. J. Bunge, in 'Directional Properties of Materials', (edited by H. J. Bunge), DGM Informationsgeselschaft-Verlag, Oberursel (1988) p.1.

[13] I. Tomov, *Phys. Stat. Sol.* (*a*) **95** 937 (1986); **98** (1986) 43.

[14] I. Tomov, in 'X-ray and Neutron Structure Analysis in Materials Science', (edited by J. Hasek), Plenum, New York (1989) p. 215.

[15] R. S. Rudman, *J. Appl. Phys.* **50** (1979) 7195.

[16] A. Kolmogorov, *Bull. Acad. Sci. USSR* (*sci. math. natur.*) **3** (1937) 355.

[17] M. Avrami, *J. Chem. Phys.* **7** (1939) 1103; **8** (1940) 212; **9** (1941) 177.

[18] W. A. Johnson and R. F. Mehl, *Trans. Amer. Inst. Min.* (*Metall*) *Engrs* **135** (1939) 416.

[19] K. Meyer, Physikalisch-chemische Kristallographie, VEB Deutscher Verlag für Grundstoffindustrie, Leipzig (1968), (Russian transl., Moskwa "Metallurgia" (1972) p. 246).

[20] J. C. Fisher, *J. Appl. Phys.* **22** (1950) 74.

[21] J. Pielaszek, in 'Hydrogen Degradation of Ferrous Alloys', (edited by R. D. Friani, J. P. Hirth, M. Smialowski), New Publication Parc Ridge, USA (1985) p. 167.

[22] E. Fromm and E. Gebhardt, 'Gase und Kohlenstoff in Metallen', Springer-Verlag, Berlin (1976) p. 622.

[23] E. A Prodan, Neorganitcheskaja Topochimija, "Nauka i Technika" Minsk (1986).

[24] A. Atrens, D. Mezzanote, N. F. Fiore and A. Genshaw, *Corros. Sci.* **20** (1980) 673.

[25] R. M. Latanision and M. Kurkela, *Corrosion-Nice* **39** (1983) 174.